RC-LACE stay report

Testing the performance of Semi-Lagrangian Horizontal Diffusion (SLHD) at different horizontal resolutions

Mario Hrastinski

Supervised by: Petra Smolíková

13.5-24.5.2019. and 3.6-14.6.2019.

CHMI, Prague, Czech Republic

1 Introduction

One of the main roles of horizontal diffusion in NWP models is to remove accumulated energy near the tail of the spectrum which is trapped due to model's finite truncation, i.e. to damp short waves that do not have any predictive skill. Semi-Lagrangian Horizontal Diffusion[1],[2] (SLHD) is an alternative scheme (to Linear Spectral DIFFusion - LSDIFF) for horizontal diffusion implemented into the ALADIN/ARPEGE system. Unlike LSDIFF, which is purely a numerical tool, SLHD is constructed in a way to represent physical processes of a horizontally damping character, e.g. horizontal effects of turbulence and molecular dissipation. In order to retain acceptable numerical efficiency and to perform in agreement with physical reality, SLHD uses damping properties of Semi-Lagrangian (SL) interpolators for representation of diffusive processes.

The SLHD scheme is consisted of three components: reduced spectral diffusion, supporting spectral diffusion and grid-point diffusion. The first two components are linear diffusions used mainly to cover numerical aspects, while later one is a flow-dependent nonlinear diffusion using the properties of SL interpolators. There are many tunable parameters related to different components of the SLHD. However, the main goal of this stay is to test the performance of the grid-point component at 1 km resolution, as well as the possibility of its tuning. Concern-

ing the representation of horizontal effects of turbulence the question related to necessity of adapting SLHD for the *grey zone* of turbulence (where turbulent eddies are partly resolved and partly sub-grid) arises. To determine how close we are to the *grey zone*, resolved and sub-grid Turbulence Kinetic Energy (TKE) for 1, 2 and 4 km horizontal resolution configurations will be compared.

2 Grid-point part of the SLHD (theoretical background)

The grid-point component is essential part of the SLHD scheme. The intensity of the grid-point diffusion is computed through κ coefficient:

$$\kappa = \frac{\Delta t F(d)}{1 + \Delta t F(d)} \tag{1}$$

which depends on horizontal flow deformation function F(d) and model time-step (Δt). Horizontal flow deformation function is defined in the following way:

$$F(d) = a \cdot 2d \cdot \left(max\left[1, \frac{d}{d_0}\right]\right)^{SLHDB} \tag{2}$$

where a is the main scaling factor for grid-point diffusion, d_0 is a threshold above which enhanced diffusion is activated and SLHDB is tunable parameter for further enhancement of F(d). a and d_0 are given by following expressions to make F(d) independent of the model resolution:

$$a = SLHDA0\left(\frac{c[\Delta x]_{3,ref}}{[\Delta x]_3}\right)^{ZSLHDP1} \tag{3}$$

$$2d_0 = SLHDD00\left(\frac{c[\Delta x]_{3,ref}}{[\Delta x]_3}\right)^{ZSLHDP3} \tag{4}$$

where c is a stretching factor (c=1 for plane geometry), $[\Delta x]_{3,ref}$ is reference value of the previous ALADIN/LACE domain, while $[\Delta x]_3$ is "CFL-spectral" mesh size. Other parameters in (3) and (4) are all tunable. The role of empirical parameters ZSLHDP1 and ZSLHDP3 is to make F(d) general with respect to actual mesh and domain size. Their values have been evaluated as ZSLHDP1=1.7 and ZSLHDP3=0.6. This leaves us with three tunable parameters within the grid-point part of the SLHD: SLHDA0 (overall strength of diffusion), SLHDD00 (threshold for enhanced diffusion) and SLHDB (further enhancement of F(d) with respect to the threshold). Once when κ is computed, the strength of diffusion (or more precisely the

weight given to diffusive operator; cf. (5-6)) may be further modified by tuning SLHDKMIN (κ_{min}) and SLHDKMAX (κ_{max}) namelist parameters, i.e. the values to which κ=0 and κ=1 are assigned:

$$\kappa' = \kappa_{min} + \kappa(\kappa_{max} - \kappa_{min}), \qquad \kappa_{min} \leq \kappa' \leq \kappa_{max} \tag{5}$$

This new κ', which will for simplicity reasons hereinafter be denoted as κ, is then used as weight factor in determining the "final" interpolator (I) at the origin point of the SL trajectory[2],[3]:

$$I = I_{(1-\kappa)A+\kappa D} = I_{A+\kappa(D-A)} \tag{6}$$

where A is cubic Lagrange polynomial (accurate) and D is quadratic interpolator (diffusive).

3 Model setup

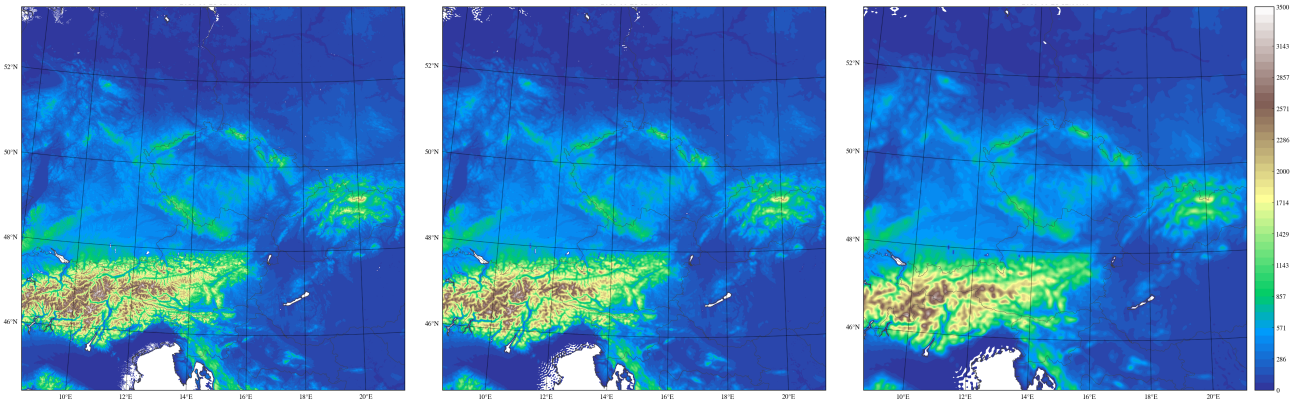

Figure 1: Orography of model domains: D1 ($\Delta x \sim 1$ km; left panel), D2 ($\Delta x \sim 2$ km; middle panel) and D4 ($\Delta x \sim 4$ km; right panel).

We utilized ALARO-CMC[4] with non-hydrostatic dynamical core and ALARO-1vB physics package (CY43t2plus-op1 version) at three domains (Figure 1.) which differ only in horizontal resolution: D1 (Δx $\sim$ 1 km; 1013 x 1013 grid points), D2 (Δx $\sim$ 2 km; 501 x 501 grid points) and D4 (Δx $\sim$ 4 km; 245 x 245 grid points). Three different configurations were initialized daily at 00 UTC during the period of intensive summer convection (21-30.06.2018.) and run throughout the 24-hours period on 87 vertical levels. The same setup was used for a strong wind case in winter (04.01.2019.), but the model was run throughout the 72-hours period to check whether there is additional accumulation of energy during longer integration period. Details regarding the reference dynamics setup and list of experiments can be found in Appendix A1.

4 Experiments with the grid-point part of SLHD

Here we present the results of numerical simulations for the case of summer convection mentioned in the previous chapter. As a main tool for an estimation of SLHD performance we utilize the Kinetic Energy (KE) spectra. However, as soon as we find larger differences in the slope of the KE spectra, we will resort to computation of verification scores.

First we compare the reference setup across different model levels and horizontal resolutions (Figure 2.). In general, the slopes of the spectra follow theoretical expectations, except near the surface where accumulation of energy is observed at the end of the $k^{-5/3}$ region (e.g. after k=100 for D101 experiment). This feature is evident during all 10 days of simulations and it is most pronounced around 12 UTC at 1 km resolution. However, during the winter simulation it was absent even during 2^{nd} and 3^{rd} day of simulation (not shown here). As a result of this feature we will focus our further experiments towards strengthening of diffusion with the goal of removing it. For comparison of the reference SLHD spectra with those for full spectral diffusion cf. Figure A2.1 in Appendix A2.

(a) level 80 **(b)** level 60 **(c)** level 20

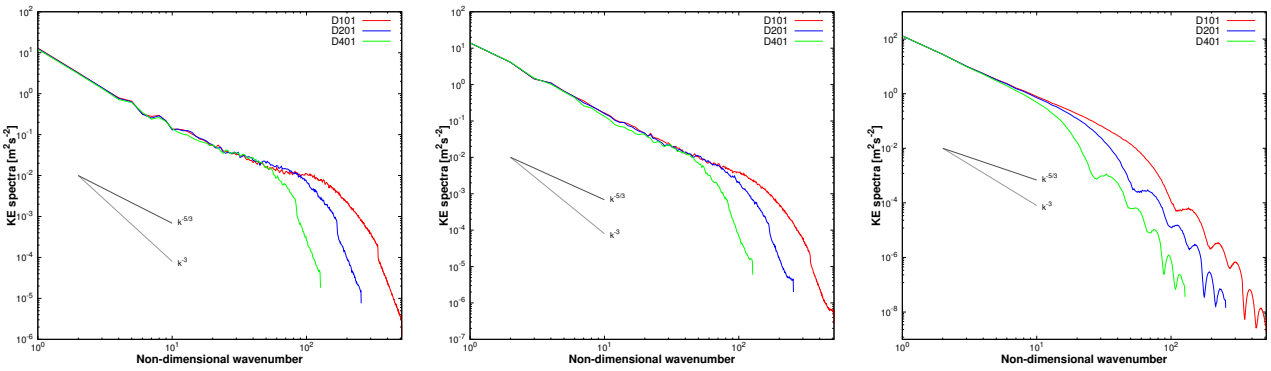

Figure 2: Kinetic energy spectra at 12 UTC 21.06.2018. for the reference setup and all domains on different model levels: level 80 (left panel), level 60 (middle panel) and level 20 (right panel).

Before the testing of tunable parameters, we did several sensitivity studies to determine the overall impact of the grid-point part of SLHD scheme, as well as some of its parts. These experiments included: i) switching-off the grid-point part of SLHD (SLHDA0=0; exp03), ii) turning-on the strongest possible grid-point diffusion ($\kappa = 1$; exp30), iii) removing the enhancement of diffusion when deformation is smaller than the threshold (d0; exp02) and iv) switching-off the d0 impact (SLHDB=0; exp04).

The values of κ coefficient for relevant experiments at different model levels are shown on Figure 3. Since κ=0 and κ=1 for exp03 and exp30, we did not plot them here. As expected, enhanc-

ing factor coming through "max" factor in (2) becomes important at higher levels (Figure 3.; upper panels) where deformation is smaller. In principal, the same is seen on spectra (Figure 4.). Moreover, from spectra we can see that impact of the grid-point part of SLHD is significant near the tail of the spectra and that spectra of the reference configuration are quite close to the one with maximum diffusion (κ=1). For 2 and 4 km configurations, this difference is bigger, so as the impact of simplifications given via exp02 and exp04.

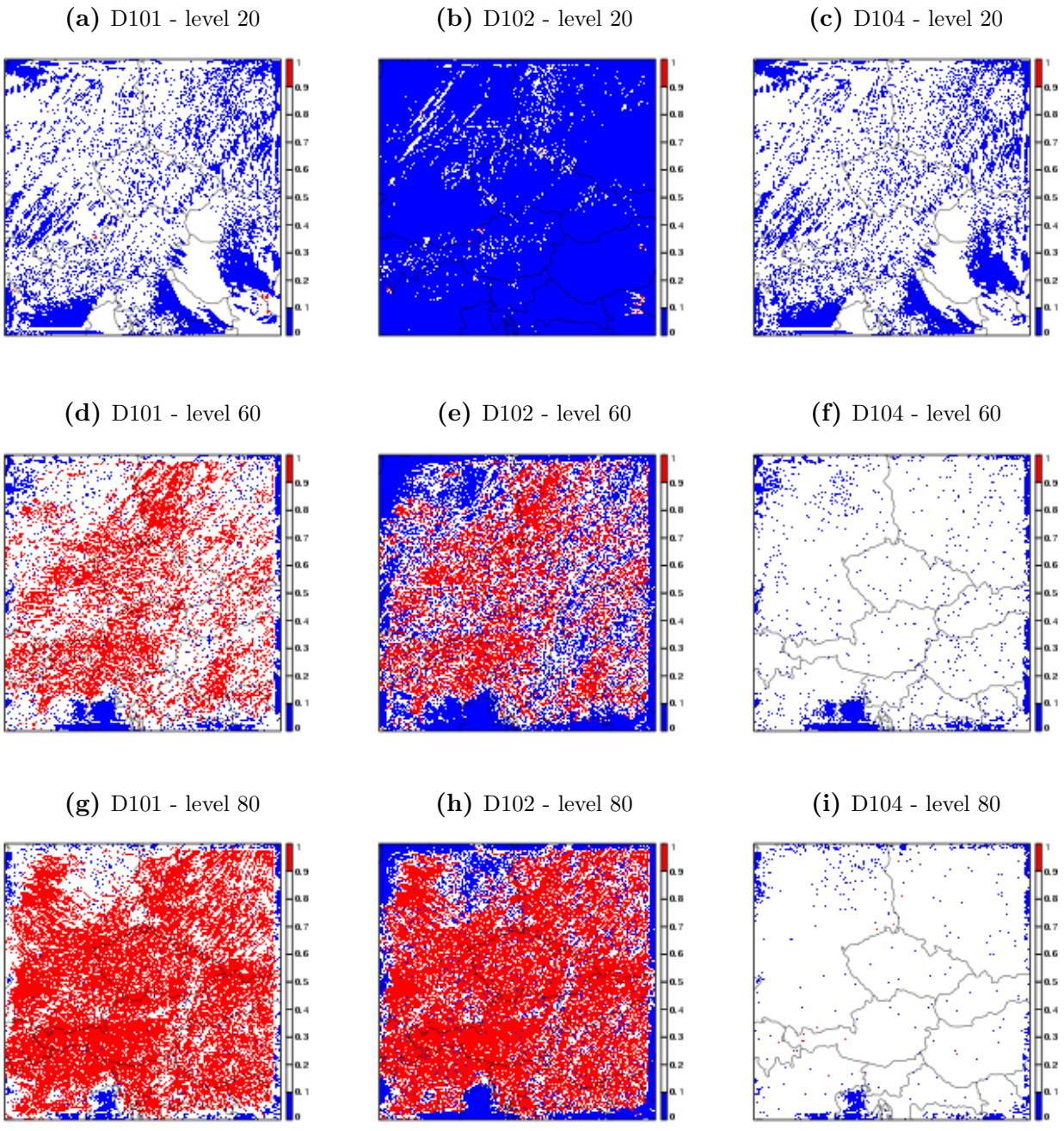

Figure 3: κ coefficient at 12 UTC 21.06.2018. for different model levels and experiments (D1 only).

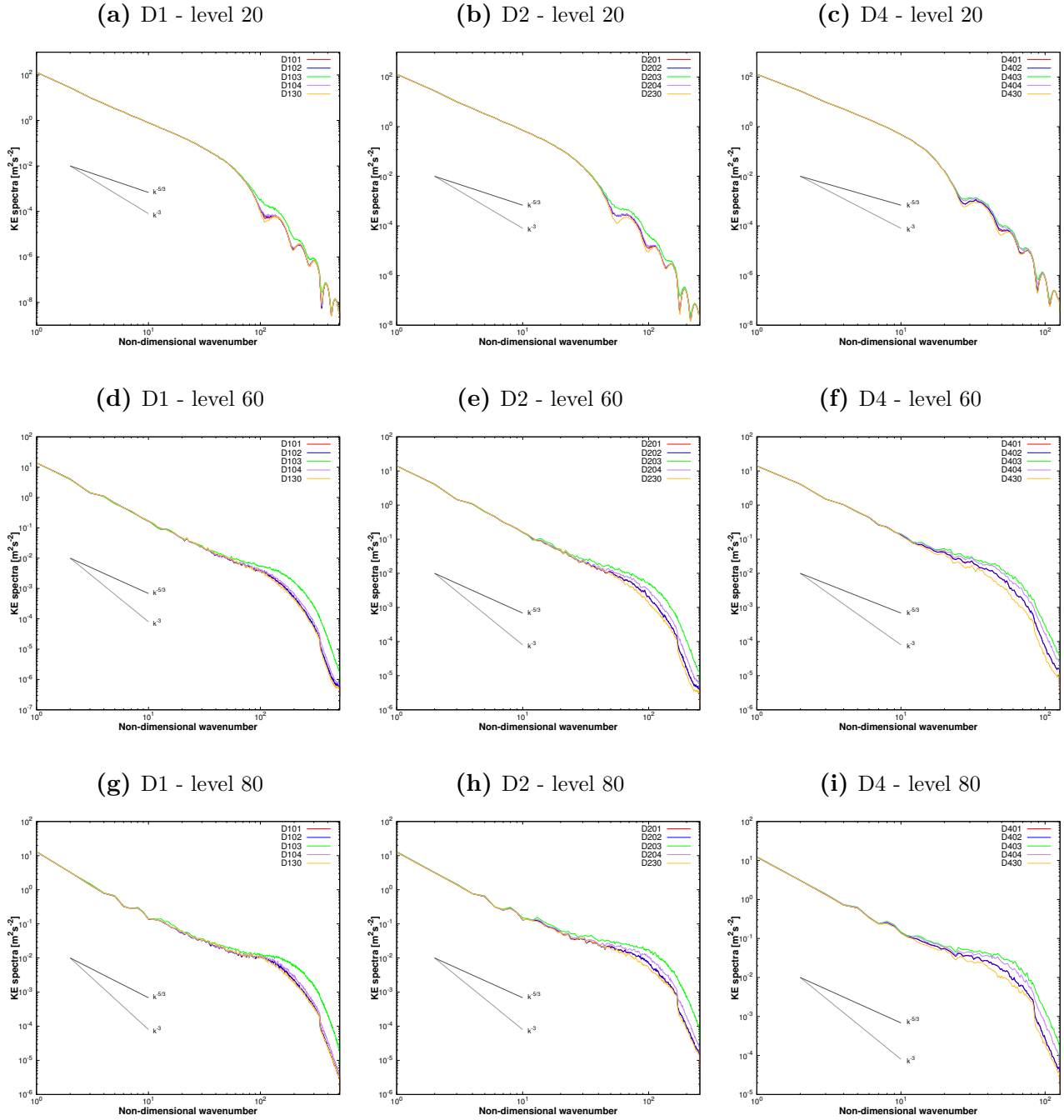

Figure 4: Kinetic energy spectra at 12 UTC 21.06.2018. for different experiments on domains: D1 ($\Delta x = 1$ km; left panel), D2 ($\Delta x = 2$ km; middle panel) and D4 ($\Delta x = 4$ km; right panel).

General conclusion, valid for all tested parameters (until now and onwards), is that higher resolution configurations show less sensitivity to their variations. We already showed that the impact of grid-point part of SLHD is significant. However, once when we reach certain value of κ coefficient, the impact with further increase is marginal (Figure 5.). In this, latest set of experiments, we compared the spectra of 1 km configuration simulations with constant κ value of 0.2 (exp18), 0.7 (exp17), 1.0 (exp30) and the reference. The scores for the later two are

shown on Figure A2.2 and A2.3 in Appendix. As stated previously the impact of increase in κ is marginal (after reaching certain value), except above 500 hPa level.

(a) level 80 **(b)** level 60 **(c)** level 20

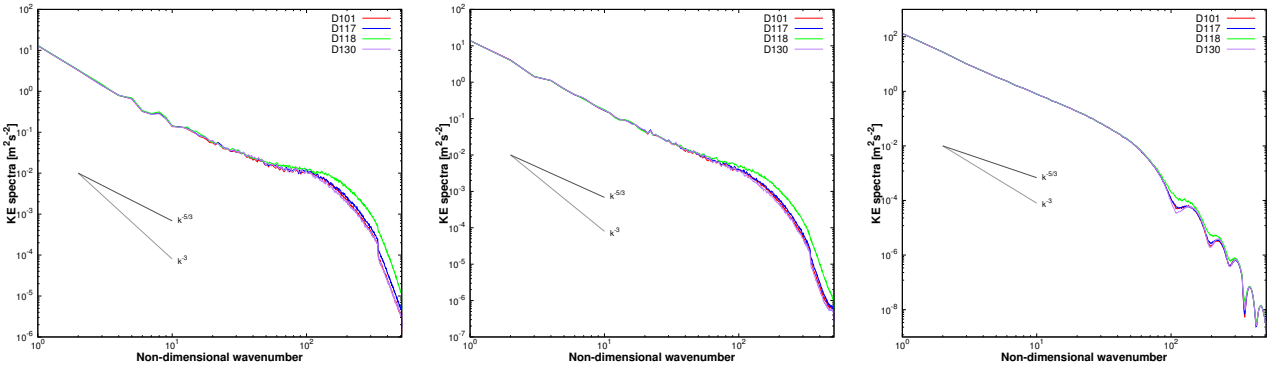

Figure 5: Domain D1 kinetic energy spectra at 12 UTC 21.06.2018. for the reference and different constant values of κ on model levels: level 80 (left panel), level 60 (middle panel) and level 20 (right panel).

From now on we focus on testing the impact of tunable parameters SLHDA0, SLHDD00, SLHDB and SLHDKMAX and their combinations. First we tested the impact of SLHDA0 varying it over several orders of magnitude (exp05-07; cf. Table 1. in Appendix A1.). The impact, both on spectra and verification scores, is practically negligible (not shown here). In terms of κ, with increase of SLHDA0 we approach more and more closer towards κ=1 everywhere. Further we tested SLHDD00 (exp08, exp10 and exp19-22). The impact on both spectra and scores is bigger than for SLHDA0, but still relatively small. In terms of κ, first two experiments led to more dichotomic distribution (more values getting either towards 0 or 1), while the later ones led to κ=1 (this must happen once when threshold is too small).

(a) level 80 **(b)** level 60 **(c)** level 20

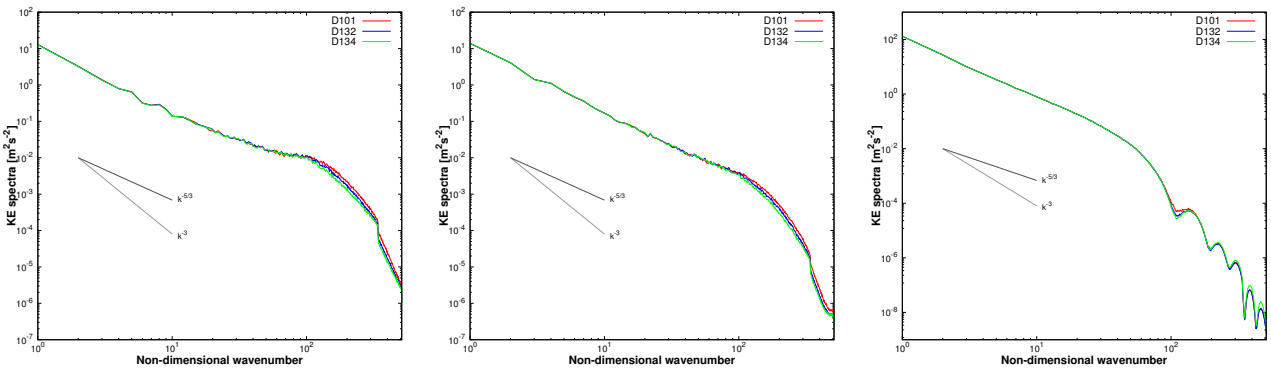

Figure 6: Domain D1 kinetic energy spectra at 12 UTC 21.06.2018. for the reference and two configurations (D132 and D134; cf. Table 1. in Appendix A1.) with combination of parameters which support enhanced diffusion: level 80 (left panel), level 60 (middle panel) and level 20 (right panel).

Regarding two other parameters, only the impact of SLHDKMAX is notable (exp23-24). However, even for maximum tested value of SLHDKMAX=12 it did not have significant impact on verification scores (not shown here). For this reason, we decided to perform tests with combination of several parameters working in the same direction of strengthening the diffusion. Out of many combinations, exp32 (SLHDD00+SLHDKMAX) and exp34 (SLHDD00+SLHDKMAX+smaller time-step) proved to be the most diffusive. Their impact on KE spectra is shown on Figure 6. However, the verification scores do not show clear signal of improvement or deterioration, i.e. below 850 hPa they are neutral or weakly improved, while in upper troposphere we observe clear deterioration (Figure A2.4 and A2.5 in Appendix A2. for exp32).

5 Experiments with supporting spectral diffusion

The Supporting Spectral DIFFusion (SSDIFF) is a very weak higher order diffusion with aim to control the small scale impact of model orography. As such, it is only applied to variables with forcing term containing orography in the prognostic equation: horizontal wind components (u and v) and vertical divergence related variable "d" (for non-hydrostatic dynamics).

(a) level 80 **(b)** level 60 **(c)** level 20

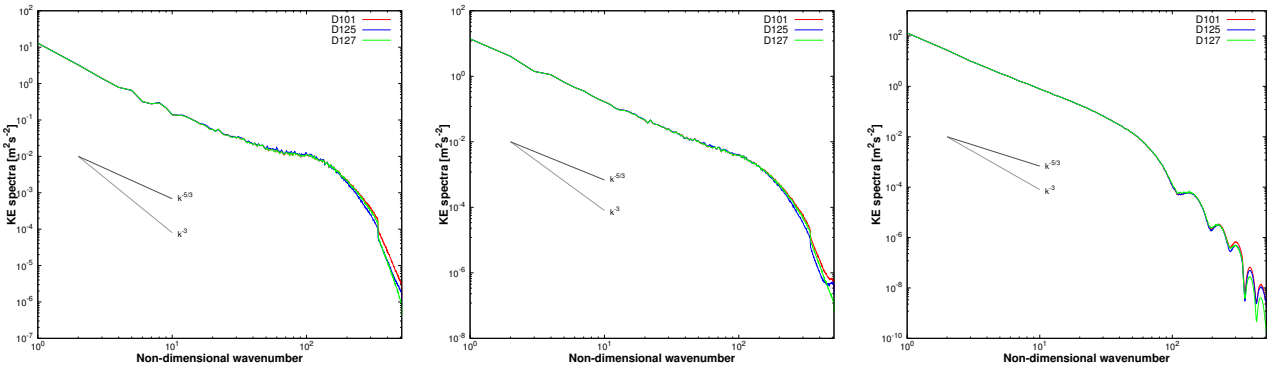

Figure 7: Domain D1 kinetic energy spectra at 12 UTC 21.06.2018. for the reference and two configurations with modified supporting diffusion for divergence (D125) and vorticity (D127) on different model levels: level 80 (left panel), level 60 (middle panel) and level 20 (right panel).

As our previous attempts to remove accumulated energy at the end of near-surface $k^{-5/3}$ region did not produce results for 1 km configuration, we decided to make two tests with parameters related to other type of diffusion which operates close to the bottom boundary, i.e. the SSDIFF. So, we increased both SSDIFF of divergence (RDAMPDIVS=2; exp25) and vorticity (RDAMPVORS=2; exp27). The signal on the KE spectra is relatively strong (Figure 7.).

However, it is present only close to the truncation point where the amount of energy is small. On the other hand, the problem we observed previously still persists.

6 Sensitivity of KE spectra to model time-step

(a) D101 - level 20 **(b)** D1292 - level 20 **(c)** D1293 - level 20

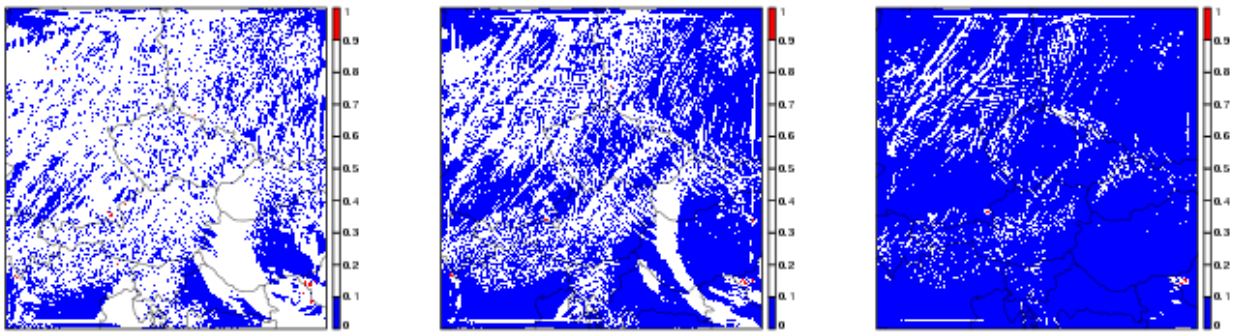

(d) D101 - level 60 **(e)** D1292 - level 60 **(f)** D1293 - level 60

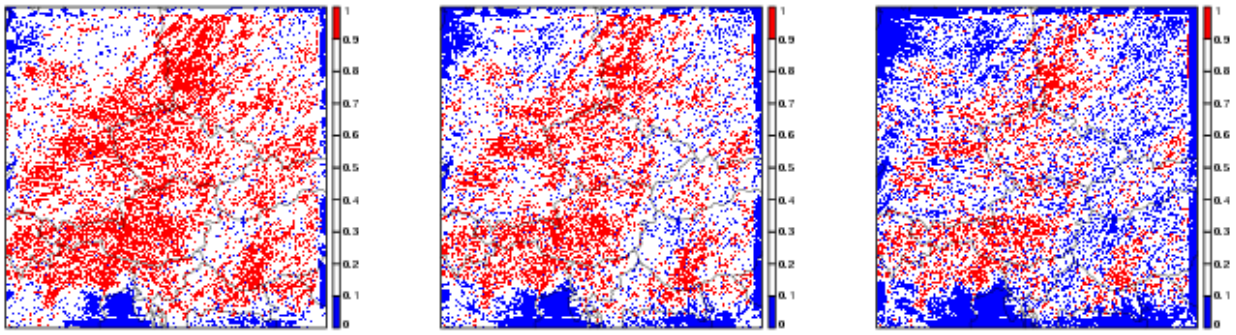

(g) D101 - level 80 **(h)** D1292 - level 80 **(i)** D1293 - level 80

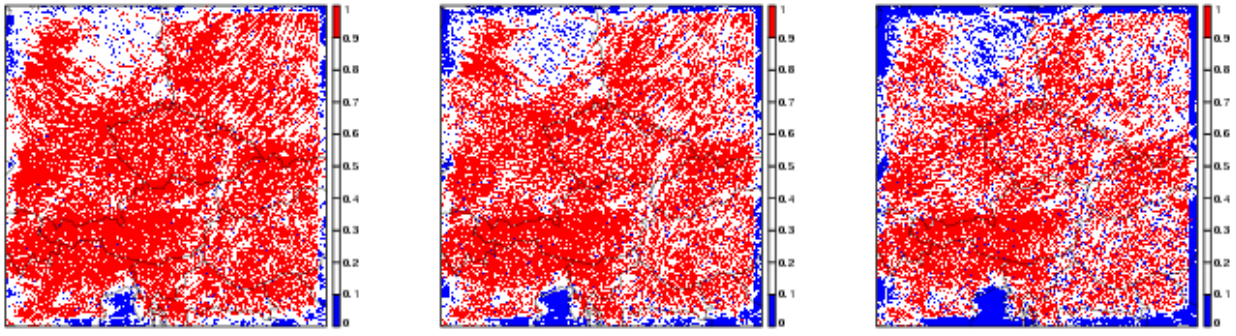

Figure 8: κ coefficient 12 UTC 21.06.2018. on different model levels and for different time-step values.

This topic is only partly related to the grid-point part of SLHD as Δt appears in (1) in role of multiplication factor for the function of the horizontal flow deformation - F(d). Given the

expression, the role of time-step in relatively weaker deformation conditions should lead to weakening of horizontal diffusion. This is exactly what we see on Figure 8., especially as we go towards higher levels where deformation has to be smaller. However, for smaller time-step there is less energy near the target region of KE spectra (Figure 9.; left and middle pannel). As this is not in accordance with κ plots (Figure 8.), we conclude that it has to come from somewhere else in the model.

(a) level 80 **(b)** level 60 **(c)** level 20

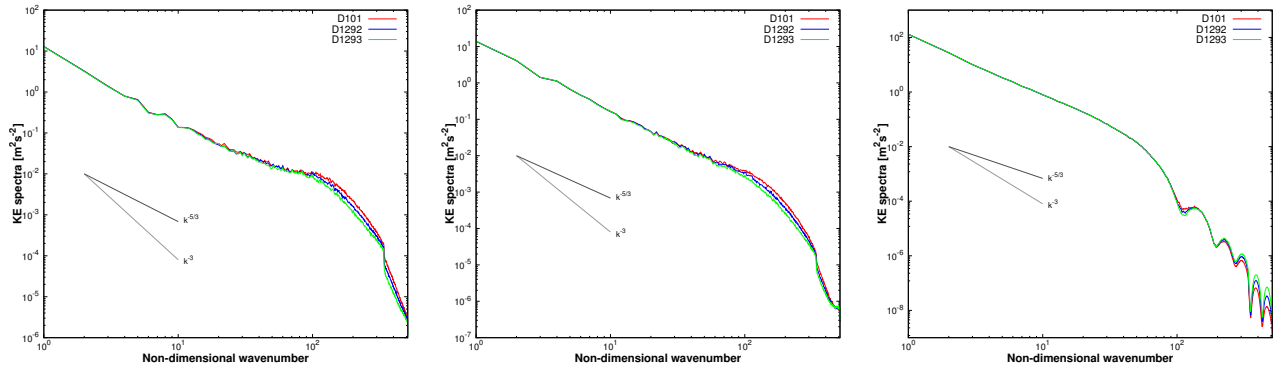

Figure 9: Domain D1 kinetic energy spectra at 12 UTC 21.06.2018. for the reference (Δt=40s) and two configurations with progressively smaller time-step values (Δt=25s for D1292 and Δt=15s for D1293) on different model levels: level 80 (left panel), level 60 (middle panel) and level 20 (right panel).

7 Computation of resolved Turbulence Kinetic Energy (TKE)

Nowadays numerical models which operate at ∼1 km horizontal resolution are able to partly resolve turbulent motions, especially in the convective Planetary Boundary Layer (PBL) [5],[6]. This zone where turbulent motions are partly resolved and partly sub-grid is called *terra incognita* or *grey zone of turbulence*. Within the *grey zone*, 1D turbulence schemes should be converted to 3D, while sub-grid part should be adequately adapted to interact with resolved. Keeping in mind that grid-point part of SLHD represents horizontal effects of turbulence, we have to think here about where ALARO-CMC is in the context of *grey zone* turbulence. For this reason we will estimate the resolved TKE (measure of turbulence intensity) and compare it to sub-grid part. According to Reynolds theory, fields can be decomposed to slow varying averages (synoptic and meso- scale) and fast varying turbulence perturbations ($\overline{u_i'}$=0):

$$u_i = \overline{u_i} + u_i' \tag{7}$$

This decomposition is only valid if there is a spectral gap between these two scales. Typically the averages are computed over some area (many grid points) and then are subtracted from

total values in individual points to obtain perturbations (e.g. [5], [7]). However, here we will apply the procedure typically used for analysis of turbulence measurements when there is a long series of measurements in a single point. So, the averages will be computed as a running average in time, i.e. 15-min in our case. For this purpose we ran all of our configurations (D1, D2 and D4) with the time-step of 15 s and thus we include 60 data in computation of the moving average (we could have gone with a larger time step, but 15 s is necessary because of the 500 m experiments whose domain is in preparation). This procedure in then repeated for each point at all model levels. Once when perturbations are computed according to (7), resolved TKE at particular grid spacing (Δx) is given by:

$$e_{res}(\Delta x) = \frac{1}{2}(u' + v' + w') \tag{8}$$

Then typically[5],[7] high resolution LES data (ideally with $\Delta x \leq 100$ m) are used with an assumption that all TKE at this resolution is resolved. Using the following expression, we can easily compute sub-grid part of TKE:

$$e^*_{tot}(\Delta x) = e_{res}(\Delta x) + e^*_{sbg}(\Delta x) \tag{9}$$

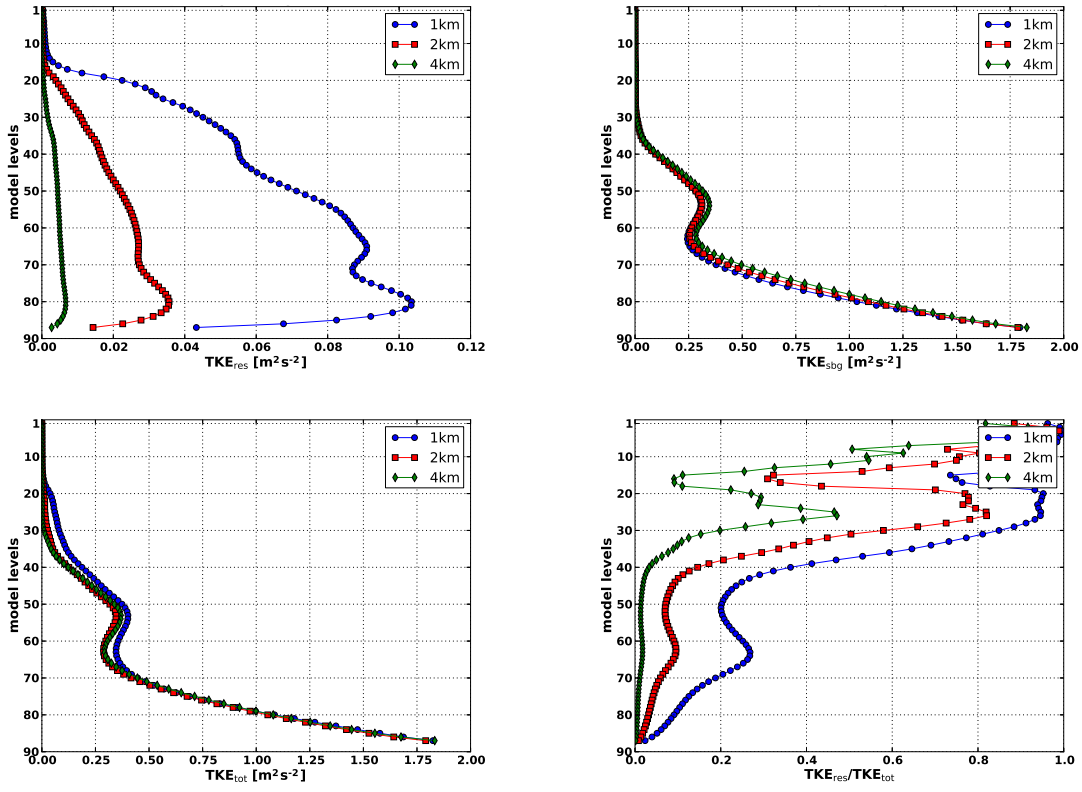

Figure 10: Spatially and temporally averaged profile of: resolved TKE (upper left panel), subgrid TKE (upper right panel), total TKE (lower left panel) and share of resolved TKE (lower right panel) for ALARO CMC 1km, 2km and 4km configurations. Time averaging interval is between 12:00 and 18:00 UTC of 21.06.2018.

Since we do not have LES data at disposal, we simply took sub-grid part as parametrized within our model. We analyzed post spin-up period of model forecast in-between +12 and +18 UTC of 21.06.2018. Spatially (over entire domain) and temporally (over 6-hours period) profiles of resolved, sub-grid and total TKE are shown on Figure 10., as well as the profile of the share of resolved TKE in total. We can freely neglect high share values above the PBL (e.g. level 50) and conclude that at 1 km resolution we enter the *grey zone* of turbulence in middle and upper PBL (bottom right panel). We should note here that even bigger share of resolved TKE is expected within the regions of strongest convection. During the analyzed case, only northern part of the domain was affected. In further analysis, we will focus on this region and shorter time frame (+15:30 to +16:30 UTC) marked at Figure 11.

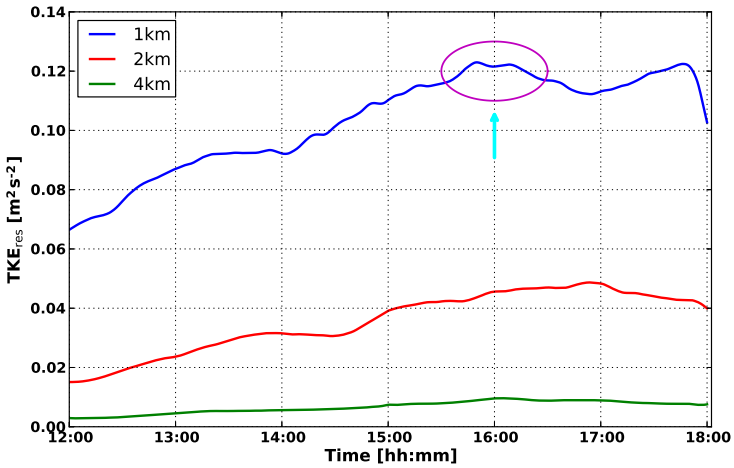

Figure 11: Spatially averaged resolved TKE for ALARO-CMC 1km, 2km and 4km configurations at model level 80 during the case of summer convection (21.06.2018.).

8 Summary and conclusion

The experiments performed during this stay confirmed the importance of SLHD, especially its grid-point part. However, it is shown that at 1 km resolution we are not able to affect the strength of diffusion, even if we apply severe options (e.g. κ =1 everywhere).

Among the analyzed tunable parameters, the greatest sensitivity was found for SLHDKMAX and SLHDD00, wherein their combination of SLHDD00=0.00018 and SLHDKMAX=10 proved as the most successful (exp32). However, the impact on scores was mixed concerning different layers of the troposphere, i.e. marginally better or neutral close to the ground and slightly worse

in upper layers. Perhaps the solution is to make grid-point part of SLHD vertically dependent. In such case, it could be achieved through SLHDD00 adapted to include certain percentage of active points at each level, i.e. not in all active regions as it is currently done. It should be noted here that the strength of Laplacian smoother (SLHDEPSH and SLHDEPSV namelist parameters) was not tested during this stay.

We also showed here that, at least in convective case, we enter the *grey zone* of turbulence at 1 km configuration. So, we should at least think about adaptation of ALARO-CMC for it. In order to achieve this, we prepared additional 500 m domain, which should together with 1 km domain serve as a basis for further research.

Acknowledgment: The author wishes to thank to Petra Smolíková for her support and cooperation, as well as to entire ONPP department for their warm welcome and hospitality. This stay is funded by the RC-LACE project.

References

[1] F. Vána. Semi-Lagrangian horizontal diffusion in ALADIN/ARPEGE. *RC-LACE report*, pages 1–13, 2006.

[2] F. Vána, P. Bénard, Simon A. Geleyn, J.-F., and Y. Seity. Semi-Lagrangian advection scheme with controlled damping: An alternative to nonlinear horizontal diffusion in a numerical weather prediction model. *Q. J. R. Meteorol. Soc.*, 134:523–537, 2008.

[3] J. Mášek. Documentation on new SLHD interpolators (introduced in ARPEGE/ALADIN cycle 35t1). *RC-LACE report*, pages 1–12, 2008.

[4] P. Termonia, C. Fischer, E. Bazile, F. Bouyssel, R. Brožková, P. Benard, B. Bochenek, D. Degrauwe, M. Derková, R. El Khatib, R. Hamdi, J. Mášek, P. Pottier, N. Pristov, Y. Seity, P. Smolíková, O. Španiel, M. Tudor, Y. Wang, C. Wittmann, and A. Joly. The ALADIN System and its canonical modelconfigurations AROME CY41T1 and ALARO CY40T1. *Geosci. Model Dev.*, 11:257–281, 2018.

[5] G. A. Efstathiou and R. J. Beare. Quantifying and improving sub-grid diffusion in the boundary-layer grey zone. *Q. J. R. Meteorol. Soc.*, 141:3006–3017, 2015.

[6] R. Honnert and V. Masson. What is the smallest physically acceptable scale for 1D turbulence schemes? *Front. Earth Sci.*, 2:1–5, 2014.

[7] R. Honnert, V. Masson, and F. Couvreux. A Diagnostic for Evaluating the Representation of Turbulence in Atmospheric Models at the Kilometric Scale. *J. Atmos. Sci.*, 68:3112–3131, 2011.

Appendix

A1. Reference dynamics setup and list of experiments

```
&NAMDYN
LADVF=.T., LQMHT=.F., LQMHW=.F., LQMP=.F., NITMP=4, NSITER=1,
NSPDLAG=3, NSVDLAG=3, NTLAG=3, NVLAG=3, NWLAG=3, RDAMPDIV=5.,
RDAMPDIVS=10., RDAMPPD=5., RDAMPQ=20., RDAMPT=20., RDAMPVD=20.,
RDAMPVDS=15., RDAMPVOR=5., RDAMPVORS=10., REPS1=0., REPS2=0.,
REPSM1=0., REPSM2=0., REPSP1=0., REXPDH=2., RRDXTAU=123.,
SDRED=1., SIPR=90000., SITR=350., SITRA=100., SLEVDH=0.5,
SLEVDHS=1., SLHDA0=0.25, SLHDB=4., SLHDD00=6.5E-05, VESL=0.,
VMAX2=280., XIDT=0.0, ZSLHDP1=1.7, ZSLHDP3=0.6
/

&NAMDYNA
LGWADV=.T., LNESC=.T., LNESCT=.F., LNESCV=.F., LPC_CHEAP=.T.,
LPC_FULL=.T., LRDBBC=.F., LSETTLS=.F., LSETTLST=.T., LSETTLSV=.T.,
LSLHD_GFL=.T., LSLHD_OLD=.F., LSLHD_SPD=.T., LSLHD_SVD=.T.,
LSLHD_T=.T., LSLHD_W=.T., ND4SYS=1, NDLNPR=1, NPDVAR=2, NVDVAR=4,
SLHDEPSH=0.016, SLHDEPSV=0.0, SLHDKMAX=6., SLHDKMIN=-0.6
/

SUDYN: LHRDI_LASTITERPC=.T.

SUDYNA: LSLHD_STATIC=.F., LSLHD_CONST=.F., RKAPPA=1.
```

Experiment number	Short description	Domains included
01	reference	D1, D2 and D4
02	reference + simplified F(d) - no max. factor	D1, D2 and D4
03	reference + SLHDA0=0	D1, D2 and D4
04	reference + SLHDB=0	D1, D2 and D4
05	reference + SLHDA0=0.7	D1, D2 and D4
06	reference + SLHDA0=2.5	D1, D2 and D4
07	reference + SLHDA0=25	D1, D2 and D4
08	reference + SLHDD00=0.0001	D1, D2 and D4
09	reference + LSLHD_STATIC=.T.	D1, D2 and D4
10	reference + SLHDD00=0.00018, 0.00020 and 0.00026	D1, D2 and D4
11	reference + SLHDB=6	D1, D2 and D4
12	reference + SLHDD00=0.00045 + SLHDB=7	D1, D2 and D4
13	exp02 + exp10	D1, D2 and D4
14	exp09 + SLHDKMAX=5.34	D1, D2 and D4
15	exp09 + SLHDKMAX=4.02	D1, D2 and D4
16	exp09 + κ=0.7	D1, D2 and D4
17	LSLHD_CONST=.T. and κ=0.7	D1, D2 and D4
18	LSLHD_CONST=.T. and κ=0.2	D1, D2 and D4
19	reference + SLHDD00=10^{-11}	D1, D2 and D4
20	reference + SLHDD00=10^{-8}	D1, D2 and D4
21	reference + SLHDD00=10^{-7}	D1, D2 and D4
22	reference + SLHDD00=10^{-6}	D1, D2 and D4
23	reference + SLHDKMAX=9	D1, D2 and D4
24	reference + SLHDKMAX=12	D1, D2 and D4
25	reference + RDAMPDIVS=2	D1, D2 and D4
26	Pure spectral diffusion	D1, D2 and D4
27	reference + RDAMPVORS=2	D1, D2 and D4
28	exp10 + SLHDB=2	D1, D2 and D4
29	reference + different time-step values	D1, D2 and D4
30	LSLHD_CONST=.T. and κ=1.0	D1, D2 and D4
31	exp28 + SLHDKMAX=10	D1, D2 and D4
32	exp10 + SLHDKMAX=10	D1, D2 and D4
33	reference + LRHDI_LASTITERPC=.F.	D1, D2 and D4
34	exp32+Δt=30, 60 and 120s[2]	D1, D2 and D4
35	reference + SLHDA0=0.75 + SLHDD00=10^{-4} + SLHDKMAX=10	D1, D2 and D4

Table 1: List of SLHD related experiments with descriptions. For default values of tested parameters cf. previous page.

[2] Default time-steps for D1, D2 and D4 are Δt=40, 75 and 150s.

A2. Comparison of full spectral diffusion and reference SLHD spectra

(a) D1 - level 20 **(b)** D2 - level 20 **(c)** D4 - level 20

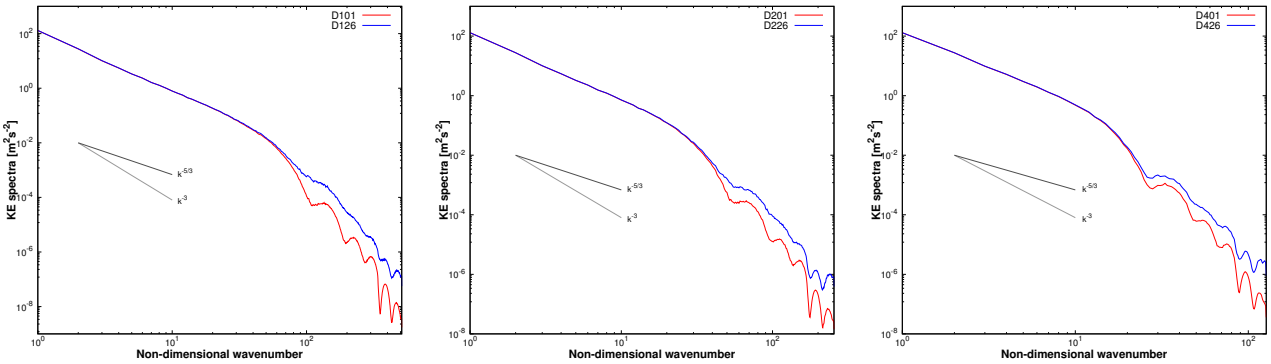

(d) D1 - level 60 **(e)** D2 - level 60 **(f)** D4 - level 60

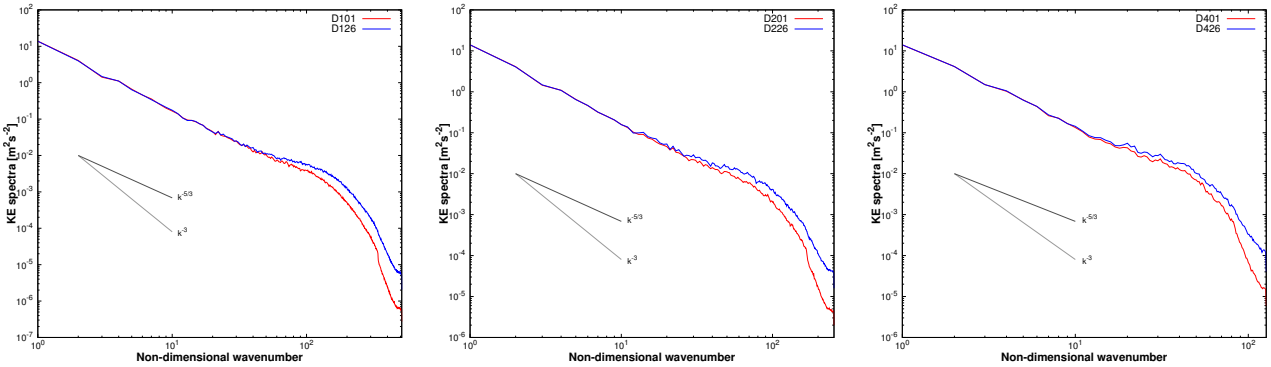

(g) D1 - level 80 **(h)** D2 - level 80 **(i)** D4 - level 80

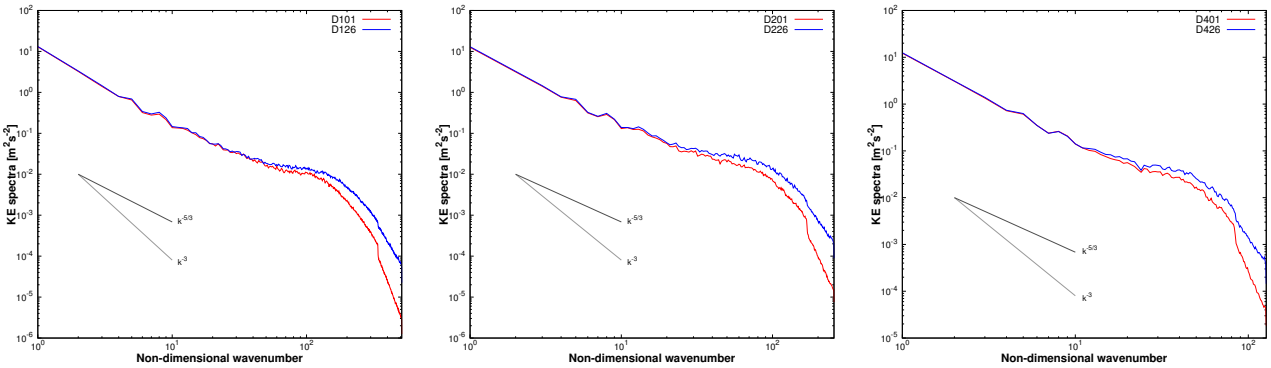

Figure A2.1: Kinetic energy spectra at 12 UTC 21.06.2018. for reference (exp01) and full spectral diffusion (exp26) on different model levels and domains: D1 (Δx = 1 km; left panel), D2 (Δx = 2 km; middle panel) and D4 (Δx = 4 km; right panel).

A3. Verification scores for selected experiments

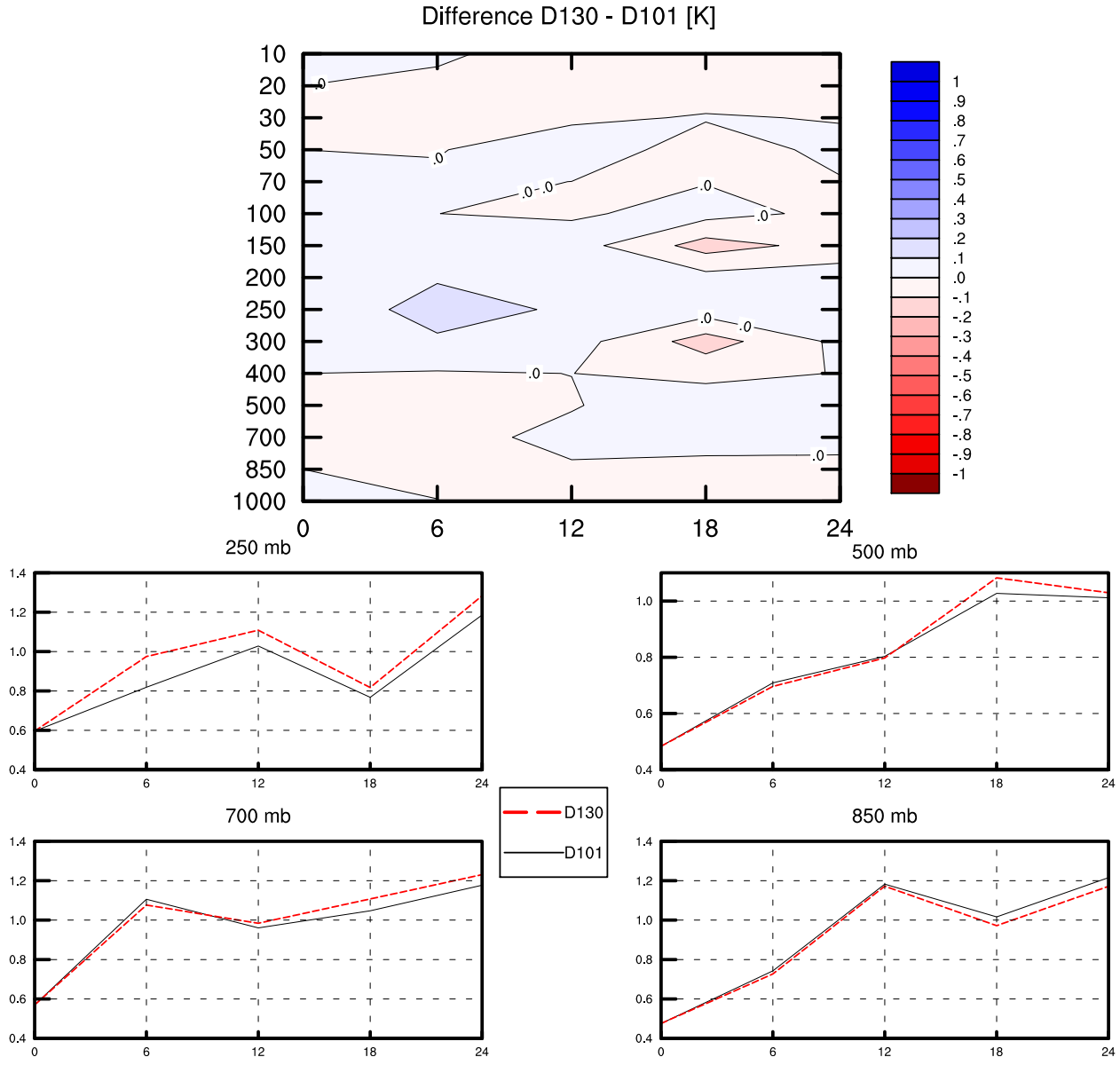

Figure A2.2: RMSE of temperature at different vertical levels for experiment (D130) and reference (D101) during the period 21-30.6.2019.

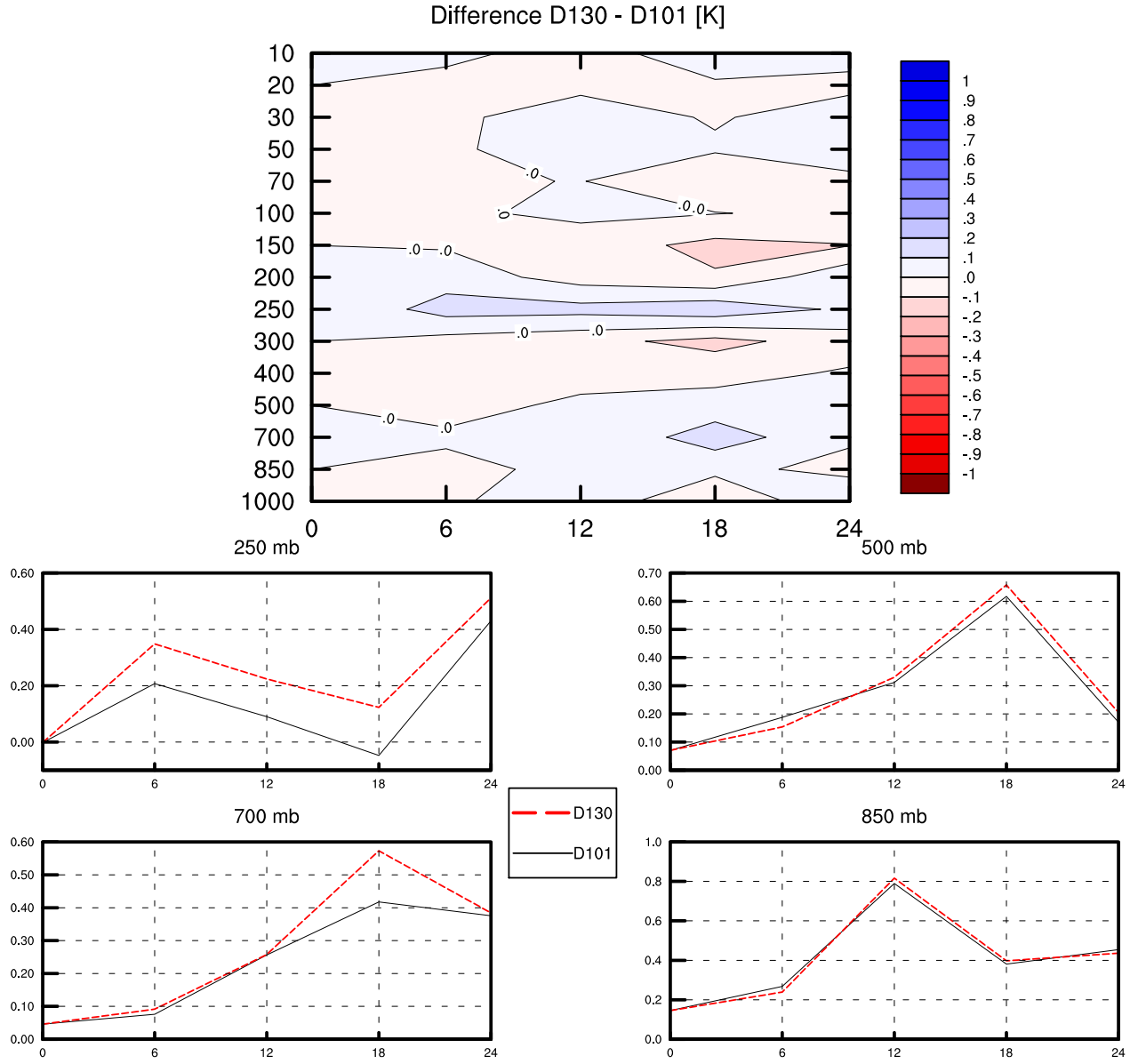

Figure A2.3: BIAS of temperature at different vertical levels for experiment (D130) and reference (D101) during the period 21-30.6.2019.

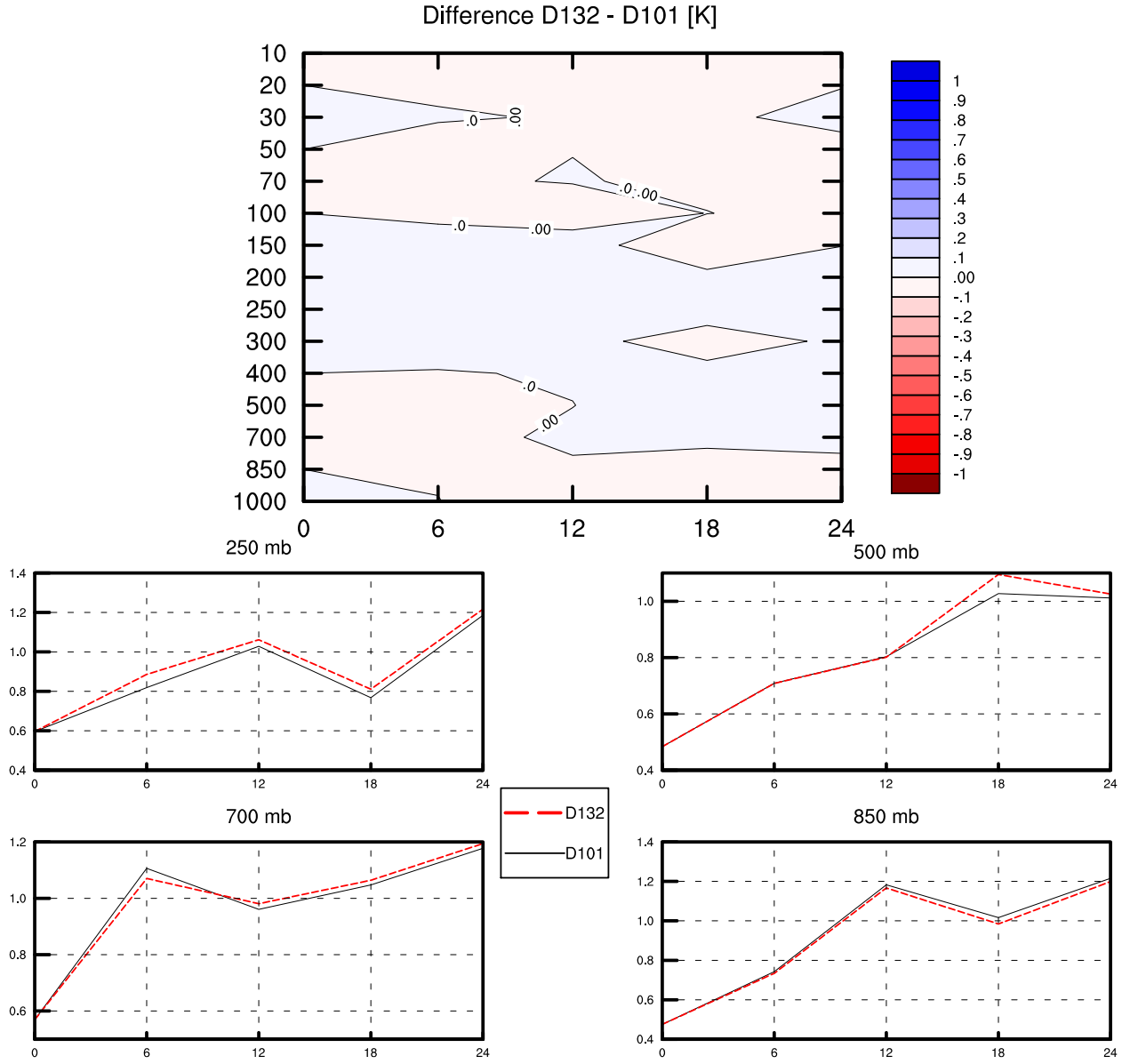

Figure A2.4: RMSE of temperature at different vertical levels for experiment (D132) and reference (D101) during the period 21-30.6.2019.

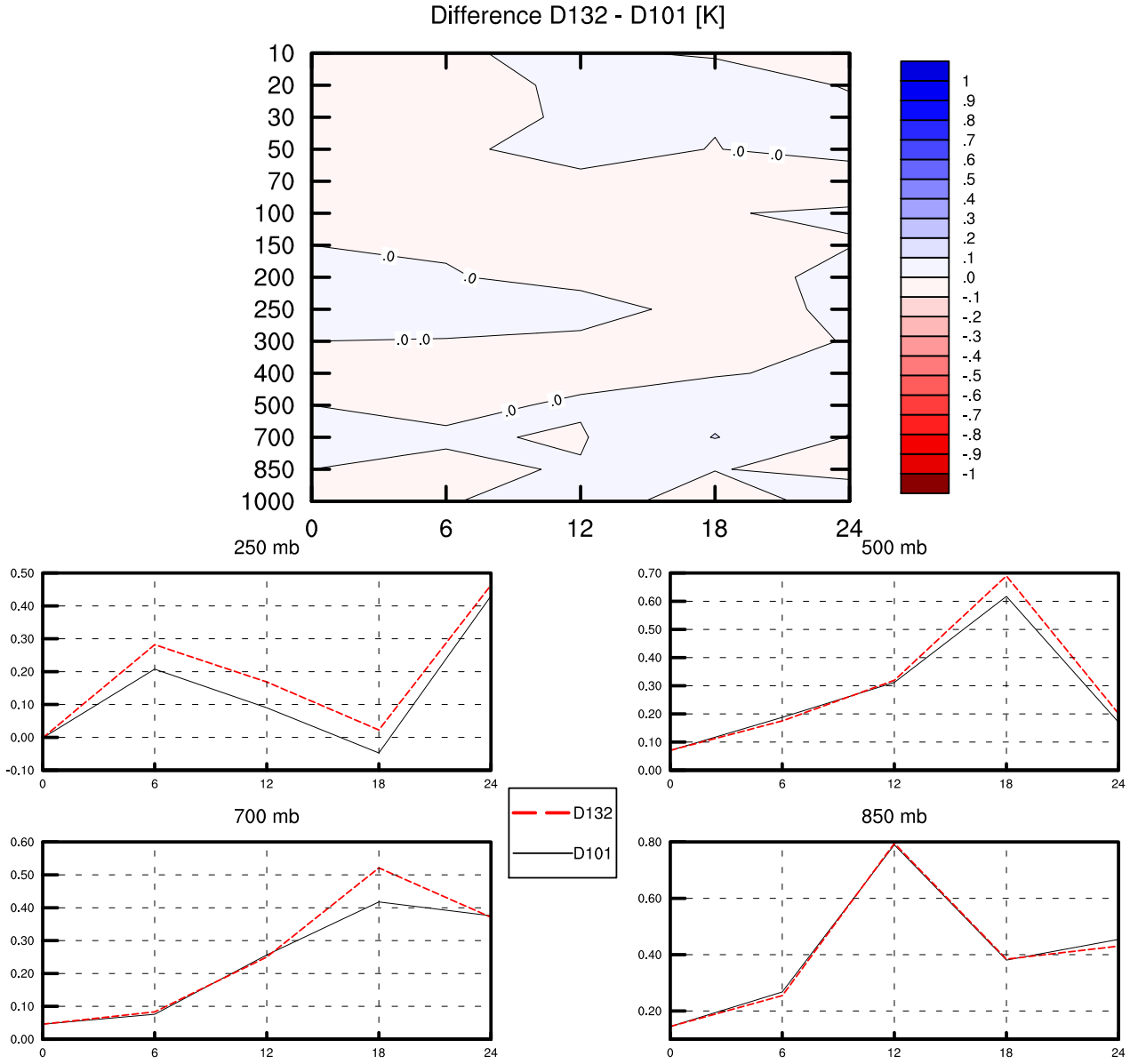

Figure A2.5: BIAS of temperature at different vertical levels for experiment (D132) and reference (D101) during the period 21-30.6.2019.